**RESEARCH REPORT**

The secretome of stressed peripheral blood mononuclear cells increases tissue survival in a rodent epigastric flap model

Stefan Hacker^{1,2} | Rainer Mittermayr³ | Denise Traxler² | Claudia Keibl³ |
Annika Resch¹ | Stefan Salminger¹ | Harald Leiss⁴ | Philipp Hacker⁵ |
Christian Gabriel^{3,6} | Bahar Golabi⁷ | Reinhard Pauzenberger¹ | Paul Slezak³ |
Maria Laggner² | Michael Mildner⁷ | Wolfgang Michlits⁸ | Hendrik J. Ankersmit^{2,9}

¹Division of Plastic and Reconstructive Surgery, Medical University of Vienna, Vienna, Austria²Christian Doppler Laboratory for Cardiac and Thoracic Diagnosis and Regeneration, Vienna, Austria³Ludwig Boltzmann Institute for Experimental and Clinical Traumatology, Vienna, Austria⁴Division of Rheumatology, Medical University of Vienna, Vienna, Austria⁵Department of Oral- and Maxillofacial Surgery, University Clinic Sankt Poelten, Sankt Poelten, Austria⁶Department of Blood Group Serology and Transfusion Medicine, Medical University of Graz, Austria⁷Department of Dermatology, Medical University of Vienna, Vienna, Austria⁸Department of Plastic and Reconstructive Surgery, Hospital Wiener Neustadt, Wiener Neustadt, Austria⁹Division of Thoracic Surgery, Medical University of Vienna, Vienna, Austria**Correspondence**

Stefan Hacker, Division of Plastic and Reconstructive Surgery, Medical University of Vienna, Waehringer Guertel 18-20, 1090 Vienna, Austria.
Email: stefan.hacker@gmail.com

Hendrik J. Ankersmit, Division of Thoracic Surgery, Medical University of Vienna, Waehringer Guertel 18-20, 1090 Vienna, Austria.
Email: hendrik.ankersmit@meduniwien.ac.at

Funding information

Laboratory for Cardiac and Thoracic Diagnosis and Regeneration and Applied Immunology; Ludwig Boltzmann Institut für Experimentelle und Klinische Traumatologie; Medical Scientific Fund of the Mayor of the City of Vienna

Abstract

Reconstructive surgery transfers viable tissue to cover defects and to restore aesthetic and functional properties. Failure rates after free flap surgery range from 3 to 7%. Comorbidities such as diabetes mellitus or peripheral vascular disease increase the risk of flap failure up to 4.5-fold. Experimental therapeutic concepts commonly use a monocausal approach by applying single growth factors. The secretome of γ -irradiated, stressed peripheral blood mononuclear cells (PBMsec) resembles the physiological environment necessary for tissue regeneration. Its application led to improved wound healing rates and a two-fold increase in blood vessel counts in previous animal models. We hypothesized that PBMsec has beneficial effects on the survival of compromised flap tissue by reducing the necrosis rate and increasing angiogenesis. Surgery was performed on 39 male Sprague–Dawley rats (control, $N = 13$; fibrin sealant, $N = 14$; PBMsec, $N = 12$). PBMsec was produced according to good manufacturing practices (GMP) guidelines and 2 ml were administered intraoperatively at a concentration of 2.5×10^7 cells/ml using fibrin sealant as carrier substance. Flap perfusion and necrosis (as percentage of the total flap area) were analyzed using Laser Doppler Imaging and digital image planimetry on postoperative days 3 and 7. Immunohistochemical stainings for von Willebrand factor (vWF) and Vascular Endothelial Growth Factor-receptor-3

Wolfgang Michlits and Hendrik J. Ankersmit contributed equally.

This is an open access article under the terms of the Creative Commons Attribution License, which permits use, distribution and reproduction in any medium, provided the original work is properly cited.

© 2020 The Authors. *Bioengineering & Translational Medicine* published by Wiley Periodicals LLC on behalf of American Institute of Chemical Engineers.

(Flt-4) were performed on postoperative day 7 to evaluate formation of blood vessels and lymphatic vessels. Seroma formation was quantified using a syringe and flap adhesion and tissue edema were evaluated clinically through a cranial incision by a blinded observer according to previously described criteria on postoperative day 7. We found a significantly reduced tissue necrosis rate (control: 27.8% \pm 8.6; fibrin: 22.0% \pm 6.2; 20.9% reduction, $p = .053$ vs. control; PBMCsec: 19.1% \pm 7.2; 31.1% reduction, $p = .012$ vs. control; 12.9% reduction, 0.293 vs. fibrin) together with increased vWF+ vessel counts (control: 70.3 \pm 16.3 vessels/4 fields at 200 \times magnification; fibrin: 67.8 \pm 12.1; 3.6% reduction, $p = .651$, vs. control; PBMCsec: 85.9 \pm 20.4; 22.2% increase, $p = .045$ vs. control; 26.7% increase, $p = .010$ vs. fibrin) on postoperative day 7 after treatment with PBMCsec. Seroma formation was decreased after treatment with fibrin sealant with or without the addition of PBMCsec. (control: 11.9 \pm 9.7 ml; fibrin: 1.7 \pm 5.3, 86.0% reduction, 0.004 vs. control; PBMCsec: 0.6 \pm 2.0; 94.8% reduction, $p = .001$ vs. control; 62.8% reduction, $p = .523$ vs. fibrin). We describe the beneficial effects of a secretome derived from γ -irradiated PBMCs on tissue survival, angiogenesis, and clinical parameters after flap surgery in a rodent epigastric flap model.

KEYWORDS

secretome, angiogenesis, flap surgery, necrosis, reconstructive surgery, tissue regeneration

1 | INTRODUCTION

Reconstructive surgery uses local, pedicled, or free flaps to restore the function and appearance after tumor resection or trauma.¹⁻³ The rate of free flap failure ranges from 3 to 7%.^{4,5} Patients requiring reconstructive surgery often suffer from diabetes mellitus or peripheral vascular disease, that were shown to increase the rate of flap failure up to 4.5-fold.⁶⁻⁹ This may lead to tissue necrosis and jeopardizes the reconstructive result. Necrosis can subsequently cause a series of events resulting in inflammation and further loss of tissue integrity.¹⁰ Experimental therapies including the use of antioxidants, vasodilators, anti-inflammatory drugs, and hyperbaric oxygen led to a decrease in necrosis rates.¹¹⁻¹⁶ Alternatively, therapeutic angiogenesis through the application of pro-angiogenic factors, such as Platelet-derived growth factor (PDGF), and Vascular Endothelial Growth Factor (VEGF) has been demonstrated to improve the survival of compromised flaps by improving tissue perfusion.^{10,17-21} The use of platelet-rich plasma (PRP) resulted in an increase in flap survival of 20% by inducing angiogenesis and reducing the inflammatory response.^{22,23} Currently, none of these therapies is used routinely during flap surgery. Fibrin sealants have been investigated for their hemostatic and adhesive properties and their ability to locally deliver and sustainably release growth factors, thus providing an important role as a biomatrix.²⁴⁻²⁸ Previous studies showed that γ -irradiated, stressed peripheral blood mononuclear cells (PBMCs) represent an easily accessible source for the production of a cellular secretome (PBMCsec) with cytoprotective, regenerative, and immunomodulatory

capacity, especially in ischemic tissues.^{29,30} In contrast to experimental therapies applying only single growth factors, PBMCsec consists of a mixture of lipids, proteins, and extracellular vesicles that together represent the regenerative potential of this cell-free therapy.³¹ Several mechanisms have already been characterized, indicating that the entire PBMCsec is required to exert its full action spectrum, as sub-fractions thereof did not reach the same beneficial effects.^{32,33} The pleiotropic effects of the secretome components better resemble the physiologic environment of wound healing occurring in the body, thus resulting in a faster and better regeneration. PBMCsec was successfully applied in animal models of wound healing, tissue ischemia or inflammation.³⁴⁻³⁹ The application of PBMCsec enhanced wound healing and angiogenesis in a murine full-thickness skin wound model. In vitro investigations showed increased migration and proliferation rates of keratinocytes, fibroblasts, and endothelial cells.³⁵ In a porcine model of burn injury, PBMCsec significantly improved the epidermal thickness, and led to a two-fold increase in angiogenesis.³⁶ The safety and tolerability of topically administered autologous PBMCsec in human dermal wounds has already been proven in a clinical phase I trial (ClinicalTrials.gov Identifier: NCT02284360).⁴⁰ An international, multi-center, randomized, double-blinded phase II clinical trial was recently initiated to investigate the regenerative effects of topically applied allogenic PBMCsec in chronic diabetic foot ulcers (ClinicalTrials.gov Identifier: NCT04277598, EudraCT number: 2018-001653-27). We hypothesized that the intraoperative application of PBMCsec leads to improved flap survival and increased angiogenesis. In contrast to previous experimental therapies, the pleiotropic effects of PBMCs resemble

the physiologic wound healing environment resulting in increased regeneration, decreased inflammation, improved microvascular perfusion, and advanced angiogenesis.

2 | RESULTS

2.1 | Treatment with PBMCsec reduces flap necrosis

The relative area of necrosis compared to the flap size was significantly reduced through the intraoperative application of PBMCsec. On day 7 after surgery, we found a complete demarcation of the necrotic area in the preoperatively defined ischemic area of the flap. Comparing the groups, the size of the necrotic areal was $27.8\% \pm 8.6$ in the control group, $22.0\% \pm 6.2$ in the fibrin group (20.9% reduction, $p = .053$ vs. control), and $19.1\% \pm 7.2$ in the PBMCsec group (31.1% reduction, $p = .012$ vs. control; 12.9% reduction, 0.293 vs. fibrin). (Figure 1a,b, Table 1).

2.2 | Treatment with fibrin sealant and PBMCsec markedly reduces postoperative seroma formation

The mean seroma volume was significantly higher in the control group ($11.9 \text{ ml} \pm 9.7$) compared to the fibrin ($1.7 \text{ ml} \pm 5.3$, 86.0% reduction, 0.004 vs. control) and the PBMCsec group ($0.6 \text{ ml} \pm 2.0$, 94.8% reduction, $p = .001$ vs. control; 62.8% reduction, $p = .523$ vs. fibrin). (Figure 1c, Table 1) Consequently, the extent of flap adherence was considerably improved in both treatment groups, especially in the clinically relevant transition and ischemic zones. In the vital zone, the extent of flap adherence was 0.46 ± 0.52 in the control group, 0.71 ± 0.91 in the fibrin group (54.3% increase, $p = .685$ vs. control), and 1.00 ± 1.21 in the PBMCsec group (117.4% increase, $p = .437$ vs. control; 40.8% increase, $p = .631$ vs. fibrin). In the transition zone, the extent of flap adherence was 0.54 ± 0.66 in the control group, 1.29 ± 0.91 in the fibrin group (138.9% increase, $p = .038$ vs. control), and 1.58 ± 0.79 in the PBMCsec group (192.6% increase, $p = .004$ vs. control; 22.5% increase, $p = .432$ vs. fibrin) In the ischemic zone, the extent of flap adherence was 0.62 ± 0.77 in the control group, 2.36 ± 0.93 in the fibrin group

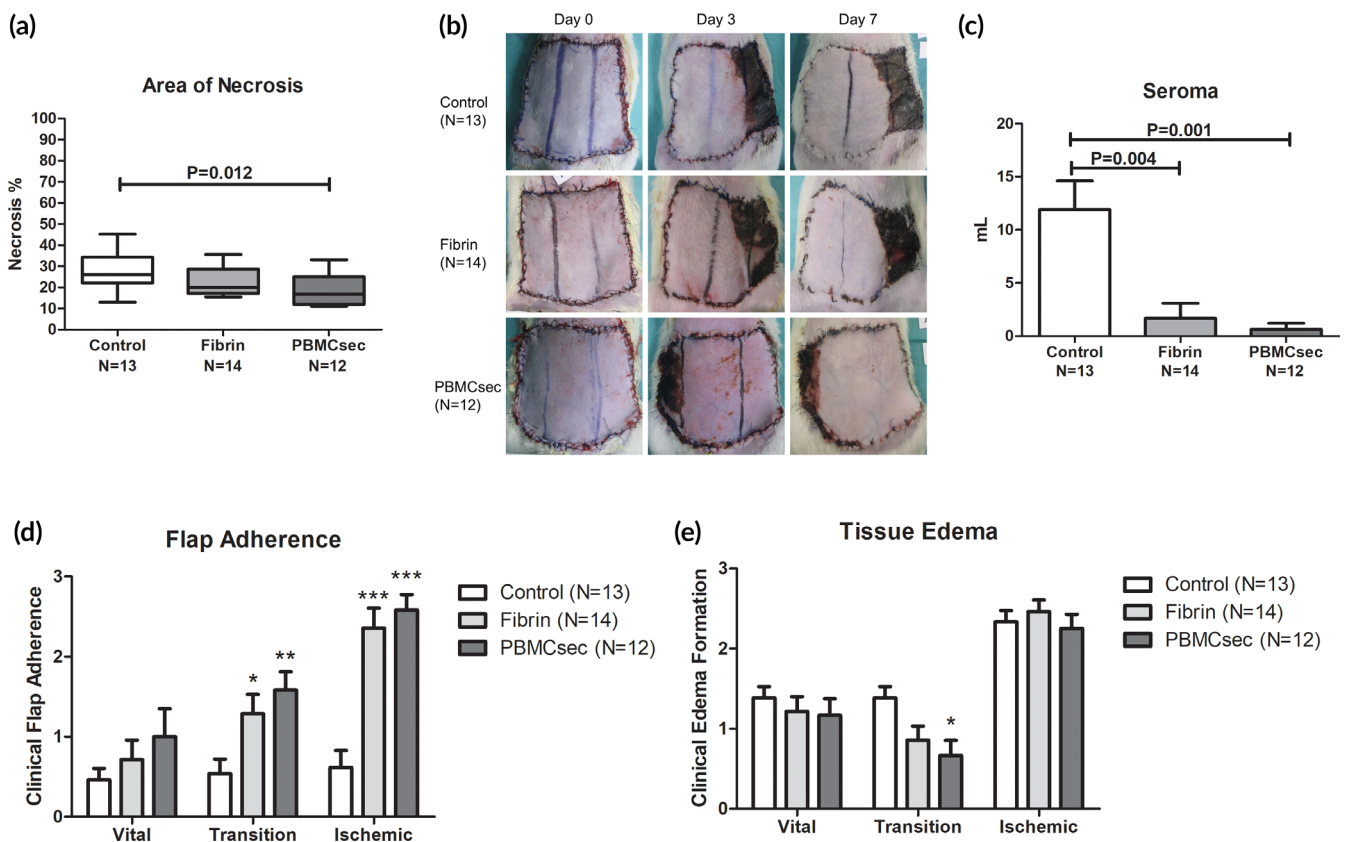


FIGURE 1 (a) The tissue necrosis rate was significantly reduced after a single, intraoperative application of the secretome derived from γ -irradiated PBMCs (PBMCsec). Only the combinatory use of fibrin and PBMCsec showed significantly improved results. (b) Examples for the development of tissue necrosis over the postoperative period are shown for each group. (c) Seroma formation was evaluated on postoperative day 7. The use of fibrin sealant alone or in combination with PBMCsec significantly reduced the volume of seroma found in the surgical wounds. Results are given as mean \pm SEM. (d) Flap adherence to the underlying tissue was evaluated clinically as parameter for tissue integration. Both groups, fibrin sealant alone and in combination with PBMC secretomes, showed markedly improved rates of flap adherence on postoperative day 7. (e) Tissue edema formation was comparable between all groups. However, in the transition zone of the flap, PBMCsec treatment led to significantly reduced clinical occurrence of edema 7 days after surgery. (*, <0.05 vs. control; **, <0.01 vs. control; ***, <0.001 vs. control)

TABLE 1 Overview of all results

	Control (N = 13)	Fibrin (N = 14)	PBMCsec (N = 12)
<i>Flap necrosis (%)</i>			
Mean	27.8	22.0	19.1
SD	8.6	6.2	7.2
p-value		.053 vs. control	.012 vs. control .293 vs. fibrin
<i>Seroma (ml)</i>			
Mean	11.9	1.7	0.6
SD	9.7	5.3	2.0
p-value		.004 vs. control	.001 vs. control .523 vs. fibrin
<i>Flap adherence</i>			
<i>Vital zone</i>			
Mean	0.46	0.71	1.00
SD	0.52	0.91	1.21
p-value		.685 vs. control	.437 vs. control .631 vs. fibrin
<i>Transition zone</i>			
Mean	0.54	1.29	1.58
SD	0.66	0.91	0.79
p-value		.038 vs. control	.004 vs. control .432 vs. fibrin
<i>Ischemic zone</i>			
Mean	0.62	2.36	2.58
SD	0.77	0.93	0.67
p-value		<.001 vs. control	<.001 vs. control .631 vs. fibrin
<i>Tissue edema</i>			
<i>Vital zone</i>			
Mean	1.38	1.21	1.17
SD	0.51	0.70	0.72
p-value		.616 vs. control	.538 vs. control .899 vs. fibrin
<i>Transition zone</i>			
Mean	1.38	0.86	0.67
SD	0.51	0.66	0.65
p-value		.068 vs. control	.016 vs. control .527 vs. fibrin
<i>Ischemic zone</i>			
Mean	2.33	2.46	2.25
SD	0.49	0.52	0.62
p-value		.611 vs. control	.843 vs. control .470 vs. fibrin
<i>Flap perfusion (PU)</i>			
<i>Transition zone</i>			
<i>Preoperative</i>			
Mean	466.9	448.6	463.0
SD	113.6	75.5	88.1

TABLE 1 (Continued)

	Control (N = 13)	Fibrin (N = 14)	PBMCsec (N = 12)
<i>Postoperative day 3</i>			
Mean	525.9	564.5	612.6
SD	140.5	86.5	217.1
p-value	.292 vs. pre	.001 vs. pre	.026 vs. pre
<i>Postoperative day 7</i>			
Mean	664.6	777.8	726.4
SD	229.6	170.6	183.7
p-value	.032 vs. pre .046 vs. day 3	<.001 vs. pre <.001 vs. day 3	.003 vs. pre .186 vs. day 3
<i>Ischemic zone</i>			
<i>Preoperative</i>			
Mean	427.6	400.5	439.1
SD	100.8	46.0	70.0
<i>Postoperative day 3</i>			
Mean	135.1	123.1	138.6
SD	46.2	41.5	63.3
p-value	<.001 vs. pre	<.001 vs. pre	<.001 vs. pre
<i>Postoperative day 7</i>			
Mean	174.1	198.9	257.6
SD	83.4	144.0	154.7
p-value	<.001 vs. pre .038 vs. day 3	<.001 vs. pre .057 vs. day 3	.007 vs. pre .017 vs. day 3
<i>vWF+ blood vessels/ 4 fields (N)</i>			
Mean	70.3	67.8	85.9
SD	16.3	12.1	20.4
p-value		.651 vs. control	.045 vs. control .010 vs. fibrin
<i>Flt-4+ cells/ 4 fields (N)</i>			
Mean	98.2	74.5	111.0
SD	53.2	46.0	66.2
p-value		.227 vs. control	.597 vs. control .112 vs. fibrin

(280.6% increase, $p < .001$ vs. control), and 2.58 ± 0.67 in the PBMCsec group (316.1% increase, $p < .001$ vs. control; 9.3% increase, $p = .631$ vs. fibrin; Figure 1d, Table 1) In the transition zone of the flap, the amount of tissue edema was shown to be significantly less pronounced in the PBMCsec group compared to the control group. In the vital zone, the extent of tissue edema was 1.38 ± 0.51 in the control group, 1.21 ± 0.70 in the fibrin group (12.3% reduction, $p = .616$ vs. control), and 1.17 ± 0.72 in the PBMCsec group (15.2% reduction, $p = .538$ vs. control; 3.3% reduction, 0.899 vs. fibrin). In the transition zone, the

extent of tissue edema was 1.38 ± 0.51 in the control group, 0.86 ± 0.66 in the fibrin group (37.7% reduction, 0.068 vs. control), and 0.67 ± 0.65 in the PBMsec group (51.4% reduction, $p = .016$ vs. control; 22.1% reduction, $p = .527$ vs. fibrin). In the ischemic zone, the extent of tissue edema was 2.33 ± 0.49 in the control group, 2.46 ± 0.52 in the fibrin group (5.6% increase, $p = .611$ vs. control), and 2.25 ± 0.62 in the PBMsec group (3.4% reduction, 0.843 vs. control; 8.5% reduction, $p = .470$ vs. fibrin; Figure 1e, Table 1).

2.3 | Flap perfusion only partially recovers to preoperative values in the ischemic zone

In the transition zone of the flap, the perfusion units measured by LDI showed a steady increase from preoperative values to postoperative

day 7. The strongest change overall was shown in the fibrin group, whereas the increase was markedly weaker in the control group. In the control group, LDI values (perfusion units) were 466.9 ± 113.6 preoperatively, 525.9 ± 140.5 on postoperative day 3 (12.7% increase, $p = .292$ vs. preoperative), and 664.6 ± 229.6 on postoperative day 7 (42.3% increase, $p = .032$ vs. preoperative; 26.4% increase, $p = .046$ vs. day 3). In the fibrin group, LDI values were 448.6 ± 75.5 preoperatively, 564.5 ± 86.5 on postoperative day 3 (25.1% increase, $p = .001$ vs. preoperative), and 777.8 ± 170.6 on postoperative day 7 (73.3% increase, $p < 0.001$ vs. preoperative; 37.8% increase, $p < 0.001$ vs. day 3). In the PBMsec group, LDI values were 463.0 ± 88.1 preoperatively, 612.6 ± 217.1 on postoperative day 3 (32.3% increase, $p = .026$ vs. preoperative), and 726.4 ± 183.7 on postoperative day 7 (56.9% increase, $p = .003$ vs. preoperative; 18.6% increase, $p = .186$ vs. day 3) (Figure 2a,b, Table 1).

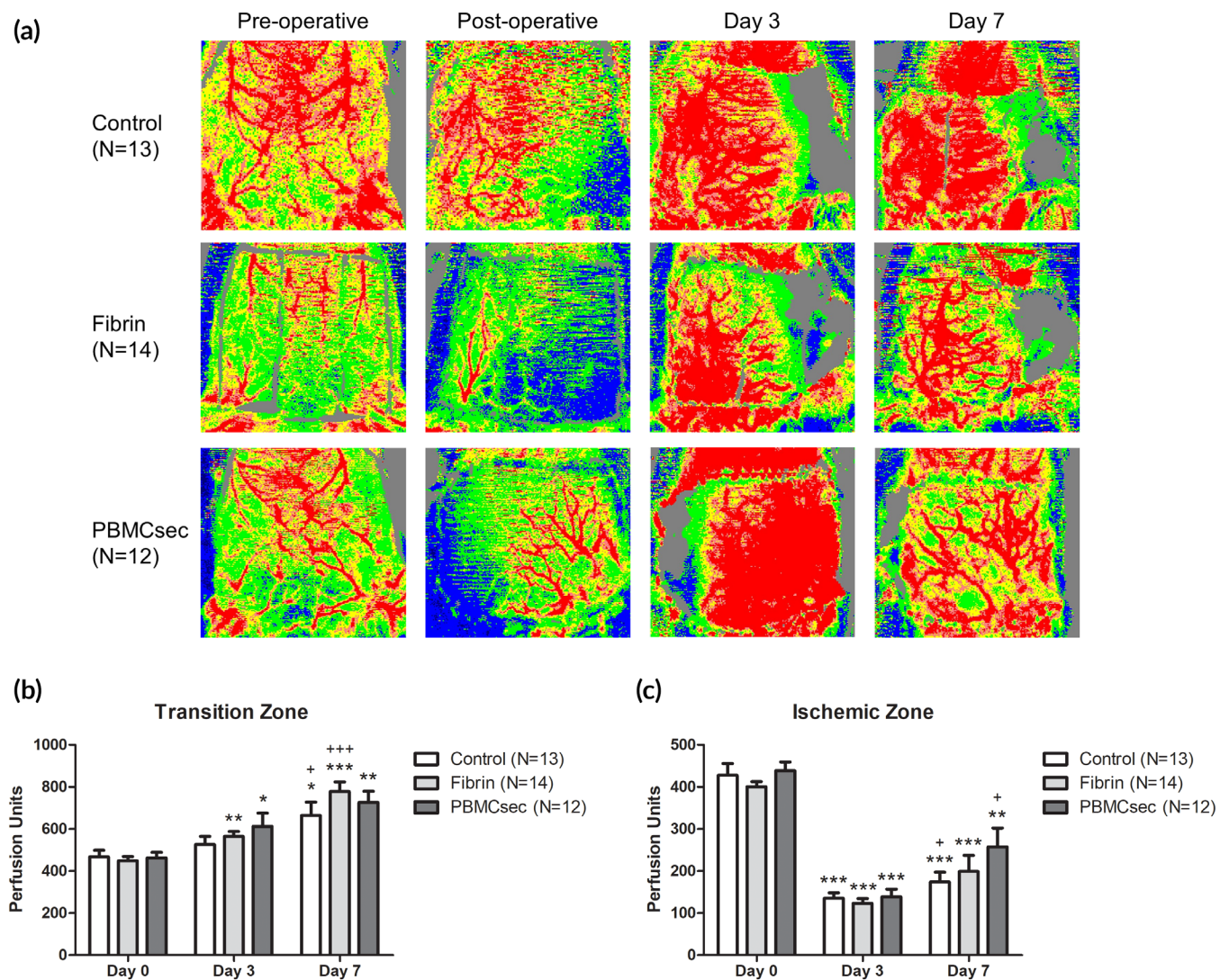


FIGURE 2 (a) Flap perfusion was measured using Laser Doppler Imaging (LDI). Examples for the color-coded image after perfusion measurements are given for each group. After ligation of the unilateral neurovascular bundle, the perfusion decreases on the contralateral side. (b) In the transition zone of the flap, a constant progression of tissue perfusion was found in all study groups. (c) After ligation of the contralateral inferior epigastric vessels, we evidenced a steep decline in tissue perfusion in the ischemic zone of the flap. The LDI measurements showed a significant recovery on postoperative day 7. The strongest effect was observed in the PBMsec treated animals. (*, <0.05 vs. day 0; **, <0.01 vs. day 0; ***, <0.001 vs. day 0; +, <0.05 vs. day 3; ++, <0.01 vs. day 3; +++, <0.001 vs. day 3; results are given as mean \pm SEM)

The situation appeared completely different in the ischemic zone. The decline from preoperative to postoperative values on day 3 was steep in all study groups. Here, the recovery of the flap perfusion was clearly stronger in the PBMsec group. In the control group, LDI values (perfusion units) were 427.6 ± 100.8 preoperatively, 135.1 ± 46.2 on postoperative day 3 (68.4% reduction, $p < .001$ vs. preoperative), and 174.1 ± 83.4 on postoperative day 7 (59.3% reduction, $p < .001$ vs. preoperative; 28.9% increase, $p = .038$ vs. day 3). In the fibrin group, LDI values were 400.5 ± 46.0 preoperatively, 123.1 ± 41.5 on postoperative day 3 (69.2% reduction, $p < 0.001$ vs. preoperative), and 198.9 ± 144.0 on postoperative day 7 (50.3% reduction, $p < 0.001$ vs. preoperative; 61.6% increase, $p = .057$ vs. day 3). In the PBMsec group, LDI values were 439.1 ± 70.0 preoperatively, 138.6 ± 63.3 on postoperative day 3 (68.4% reduction, $p < 0.001$ vs. preoperative), and 257.6 ± 154.7 on postoperative day 7 (41.3% reduction, $p = .007$ vs. preoperative; 85.9% increase, $p = .017$ vs. day 3) (Figure 2a,c, Table 1).

2.4 | Blood vessel density is increased in the PBMsec treated flaps

We found a statistically significant increase in blood vessels in the PBMsec group (85.9 ± 20.4 vessels/4 fields at 200 \times magnification; 22.3% increase, $p = .045$ vs. control; 26.8% increase, $p = .010$ vs. fibrin) compared to both, the control (70.3 ± 16.3) and the fibrin (67.8 ± 12.1 ; 3.6% reduction, $p = .651$ vs. control) group. (Figure 3a–d, Table 1) No difference was found in the presence of lymphatic vessels determined by cells staining positive for VEGFR-3 (control: 98.2 ± 53.2 cells/4 fields at 200 \times magnification; fibrin: 74.5 ± 46.0 ; 24.1% reduction, $p = .227$ vs. control; PBMsec: 111.0 ± 66.2 ; 13.0% increase, $p = .597$ vs. control; 49.0% increase, $p = .112$ vs. fibrin; Figure 3e–h, Table 1).

3 | DISCUSSION

We were able to demonstrate a reduced postoperative flap necrosis and a significantly improved rate of angiogenesis after flap surgery through the application of secretome derived from γ -irradiated, stressed PBMCs in combination with fibrin glue. Additionally, an improved flap adherence and reduced postoperative seroma formation were observed. The critical ischemia of the contralateral flap areas mimics the clinical situation in patients with impaired flap perfusion.^{7,41,42} Fibrin sealant is commercially available and was previously used as a carrier substance for growth factors and stem cells in animal flap models.^{24,26,43} It has gained widespread acceptance in clinical use.^{28,44–46} The combination of PBMsec at the described concentration of 2.5×10^7 cells/ml and fibrin glue may improve the flap survival rate in patients with co-morbidities who are at an increased risk for postoperative flap failure. Cost-effectiveness would be achievable through the prevention of secondary surgeries. Previous results attested the consistency of the PBMsec production process regarding its composition, content, and stability.⁴⁷ Its safety and tolerability in dermal wounds have been proven in a clinical phase I trial.^{40,48}

PBMsec was categorized as a biological medicinal product (Directive 2001/83/EC) by the regulatory authorities. A clinical phase II trial has been initiated and the approval for clinical use could be reachable within the next years. The proposed phase II clinical study is primarily based on the regulatory requirements of EMA/CHMP/ICH/731268/1998 and EMA/CMPM/ICH/286/1995.⁴⁸ Limitations of this study are the use of a small animal model. Further studies are needed to show the effects on flap necrosis in large animal models and humans. In addition, the production of PBMsec requires an adequate infrastructure to ensure the quality needed to achieve the described results.

PBMsec comprises a plethora of biologically active components including proteins, lipids, and extracellular vesicles and the mechanisms of action have been the focus of extensive research over the past years.^{30,31,33} On a cellular level, the irradiation of PBMCs augments the release of extracellular vesicles and shifts the protein, lipid, and miRNA composition of the secretome toward a regenerative phenotype.³³ In most of the studied biological processes the integrity of the entire PBMC secretome was necessary to achieve full regenerative effects as sub-fractions or single cell types did not reach the same capacity.^{32,33} Unlike previously described monocausal therapies, the effects of PBMsec can therefore be attributed to its heterogeneity, resembling the physiological environment necessary for tissue regeneration. Previously described therapies with single growth factors significantly reduced postoperative flap necrosis at a similar rate to the described results. However, these experimental therapies mainly focused on angiogenesis and therefore lack additional immunomodulatory and cytoprotective effects that may play a role in patients with co-morbidities.^{26,27} In correlation with the previously described effects in animal models of wound healing we found an increased density of vWF+ blood vessels after PBMsec treatment.^{35,36} The TNF/TNFRSF1B signaling pathway was described as the mechanism underlying the γ -irradiation-induced pro-angiogenic activity of PBMsec.³² Clinically, the impairment of flap perfusion leads to inflammation and secondary tissue damage.^{10,49} The immunomodulatory and cytoprotective effects of PBMsec were previously described in animal models of myocarditis, contact hypersensitivity, and cerebral ischemia.^{37,50,51} The reduction of postischemic inflammatory reactions may have a beneficial effect on tissue viability. The clinically relevant bactericidal activity of PBMsec was mainly attributed to the high abundance of different antimicrobial peptides in the secretome.⁵² In combination with reduced seroma formation, improved tissue edema and flap adherence, the angiogenic, cytoprotective, antibacterial, and immunosuppressive properties of PBMC secretome may therefore play an additional role in the markedly increased flap survival after surgery (Figure 4).

4 | MATERIALS AND METHODS

4.1 | Ethics statement

All animal experiments were approved by the local ethical authority of Vienna (807408/2013) and met the institutional and national

guidelines for the use and care of laboratory animals. The local ethics committee at the Medical University of Vienna (2010/034) approved blood donations by healthy volunteers. A detailed description of the study design is depicted in Figure 5.

4.2 | Production of secretome

PBMCsec was produced according to previously described methods (LOT: 399014).³⁹ In anticipation of possible future clinical

applications, the production followed GMP guidelines. This production process was shown to yield reproducible results.⁴⁷ Human PBMCs were isolated from the whole blood of healthy donors after obtaining informed consent by density gradient centrifugation. After 60-Gray γ -irradiation, the cells were cultivated for 24 hr with CellGenix GMP DC medium (Cellgenix, Freiburg, Germany) at a concentration of 2.5×10^7 cells/ml under sterile conditions. After centrifugation, the cells were discarded and the supernatant was collected and filtrated. For viral inactivation, the supernatant was treated with methylene blue (MB) plus light treatment using the Theraflex

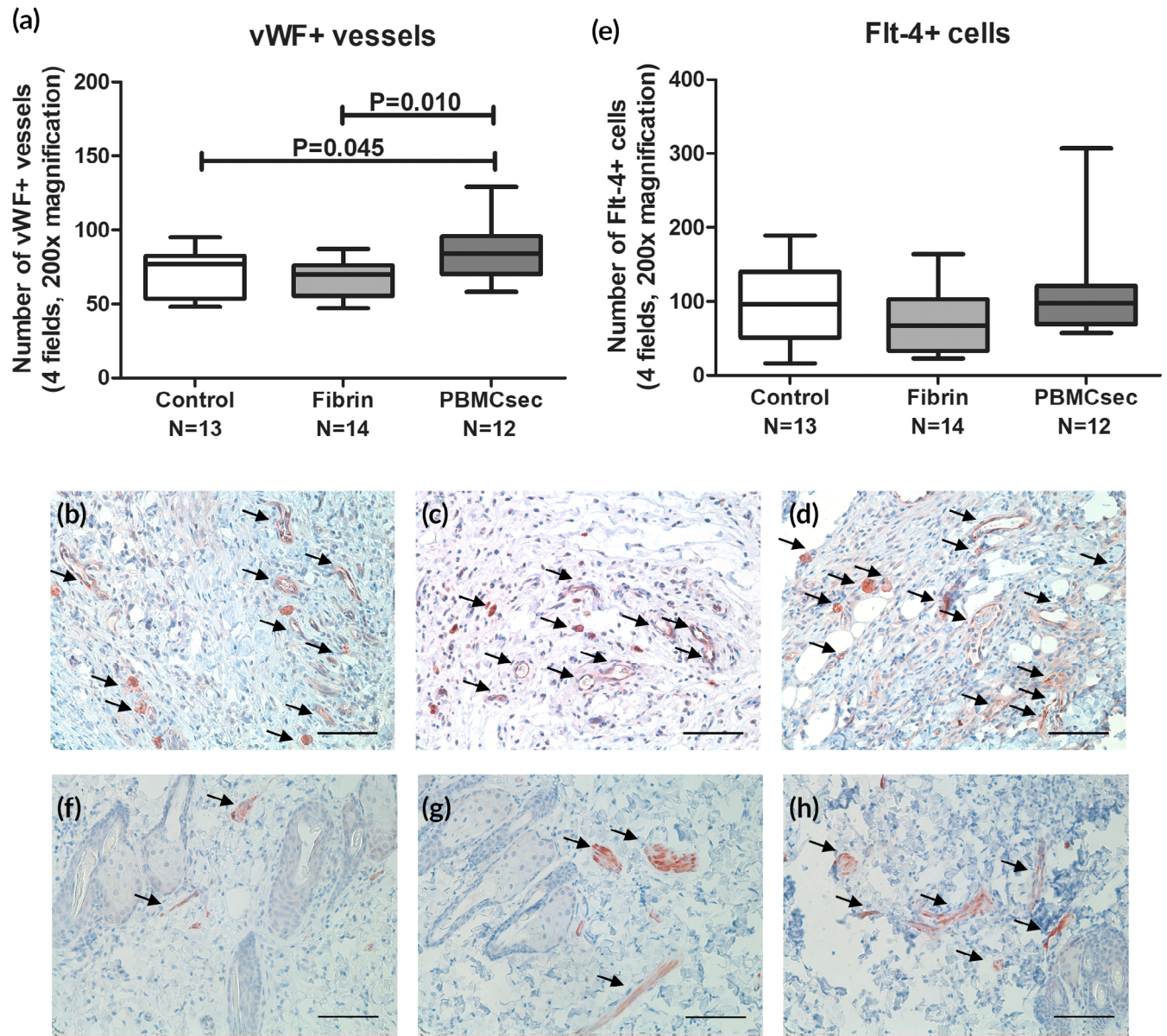


FIGURE 3 (a) The number of vWF+ blood vessels was significantly increased in the flaps treated with PBMCsec. Fibrin sealant alone did not affect blood vessel density compared to the control group. These findings are in accordance with previously published results of pro-angiogenic effects in other animal models.^{35,36} Representative stainings for vWF of control (b), fibrin (c), and PBMCsec (d) treated animals are shown. (Scale Bar = 100 μ m, arrows indicate vWF+ blood vessels) (e) Flt-4 stainings were performed to determine the effect on lymphangiogenesis in the flap tissue. We did not evidence any alterations of the Flt-4+ cell counts between the study groups. Representative stainings for Flt-4 of control (f), fibrin (g), and PBMCsec (h) treated animals are shown. (Scale Bar = 100 μ m, arrows indicate Flt-4+ cells)

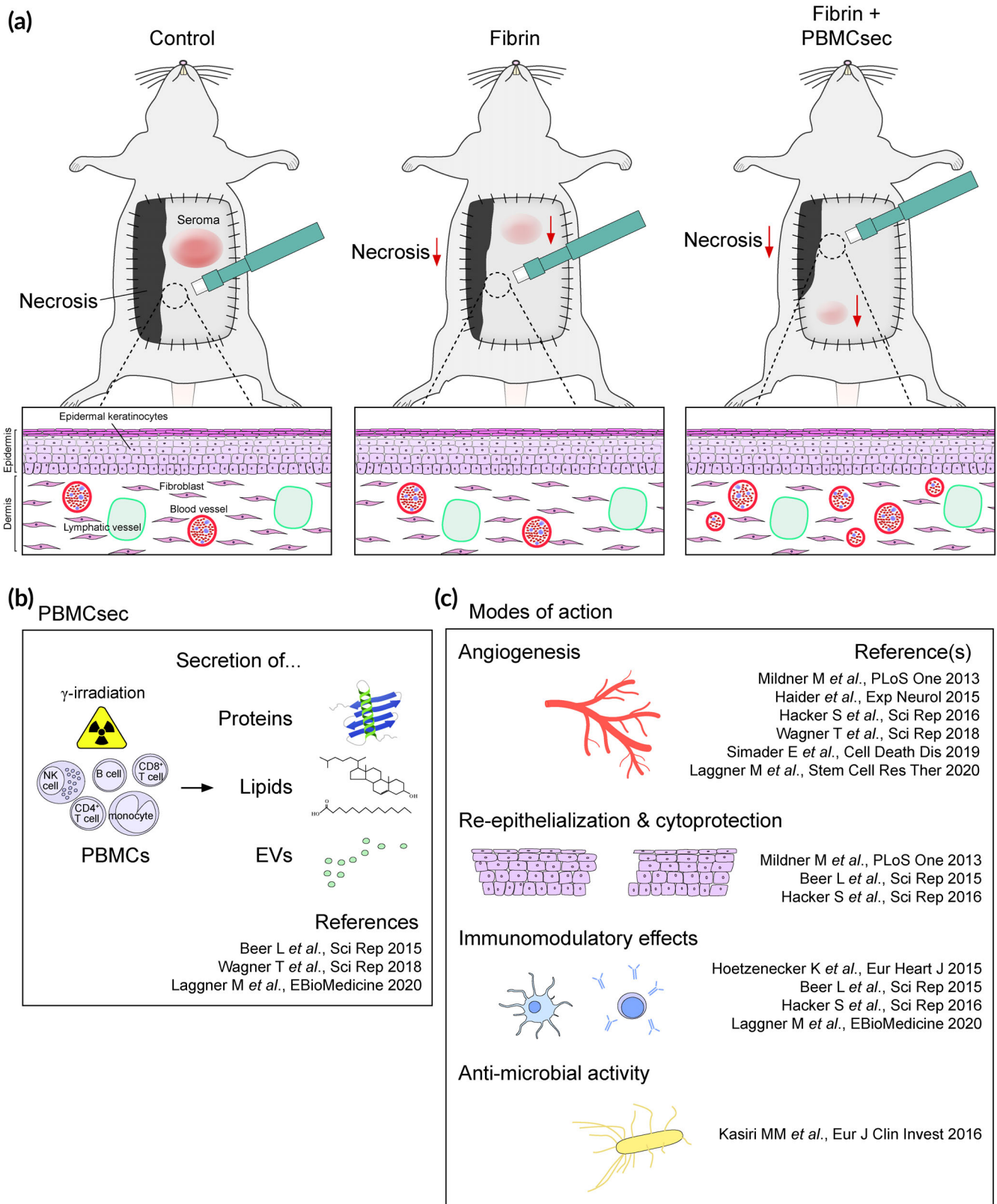


FIGURE 4 The proposed method of action for the use of PBMCsec in flap surgery is shown. (a) The intraoperative application of PBMCsec leads to a reduced rate of flap necrosis and seroma. In the tissue biopsies taken from the border between viable and necrotic tissue, increased rates of angiogenesis were found. (b) The irradiation of PBMC causes a switch toward a regenerative phenotype and induces the secretion of proteins, lipids, and EVs, which form the secretome. (c) PBMCsec resembles the physiologic environment of wound healing and regeneration and therefore has pleiotropic effects

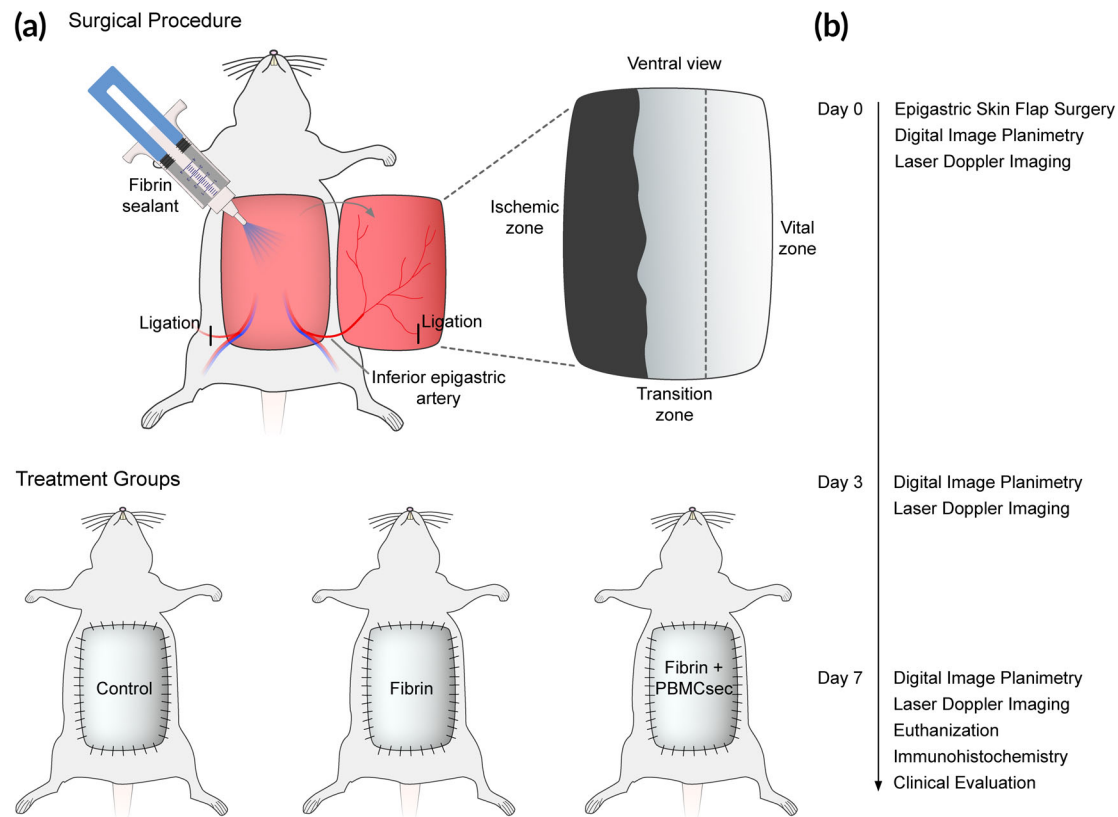


FIGURE 5 The study design and timeline are shown. Ligation of the unilateral inferior epigastric artery leads to a controlled necrosis of the contralateral side of the flap. Measurements were performed preoperatively, postoperatively, and on postoperative days 3 and 7

MB-Plasma system, the Theraflex MB-Plasma bag system, and an LED-based illumination device (MacoPharma, Langen, Germany). MB and photoproducts were removed by consecutive Blueflex filtration steps. After lyophilization of the viral-inactivated cell culture supernatant, the lyophilized powder was treated with γ -irradiation to further reduce the risk of viral contamination. The lyophilized supernatant of apoptotic PBMCs was considered pathogen-free after this two-step process and was stored at -80°C until re-suspension as needed using sterile water (Aqua ad injectabilia, B Braun, Melsungen, Germany).

4.3 | Rodent epigastric flap model

The rodent epigastric flap model was performed as described.⁴² 39 adult male Sprague-Dawley rats (weighing 422 ± 30 g) were divided in three groups according to a computerized randomization protocol (surgery without additional treatment/"control," $N = 13$; treatment with fibrin sealant/"fibrin," $N = 14$; treatment with fibrin sealant containing PBMCsec/"PBMCsec," $N = 12$). Animals were box-induced using isoflurane and maintained under general anesthesia using ketamine and xylazine. The abdomen of each animal was shaved and depilated. Animals were placed in supine position on a surgical heating pad. The borders of the epigastric skin flap were marked using previously described anatomical landmarks: cranially the xiphoid,

caudally the pubic region and bilaterally the distinct transition from the thin ventral skin to the coarse dorsal skin. This results in a flap size of approximately 8×8 cm.⁴² The flap was then divided into three distinct vertical zones: Vital zone (origin of supplying neurovascular bundle), transition zone (transition from adequate to insufficient vascular supply), and ischemic zone (area of dissected neurovascular bundle). An extended epigastric adipocutaneous flap was raised superficial to the abdominal muscular fascia from cranial to caudal. To render the contralateral part of the flap ischemic, either the left or the right inferior epigastric neurovascular bundle (according to the study randomization protocol) was ligated. The flap was sutured back to its native anatomical orientation. (Figure 6a,b) After completion of the surgical procedure, animals received analgesic therapy by subcutaneous administration of 0.05 mg/kg BW buprenorphin every 8 hr for 3 days. To prevent auto-cannibalization, the incisor teeth in the upper and lower jaw were abraded under anesthesia on the day of surgery and during dressing changes. Three and seven days postoperatively, all animals were re-anesthetized by isoflurane, digital images of the epigastric flaps were taken and the flaps were scanned using the Laser Doppler Imaging system (LDI, Moor LDI™, Moor Instruments Ltd., Devon, UK). On day 7, animals were euthanized by an overdose of pentobarbital, flaps were evaluated macroscopically, and full-thickness adipocutaneous biopsies were obtained for immunohistological analyses.

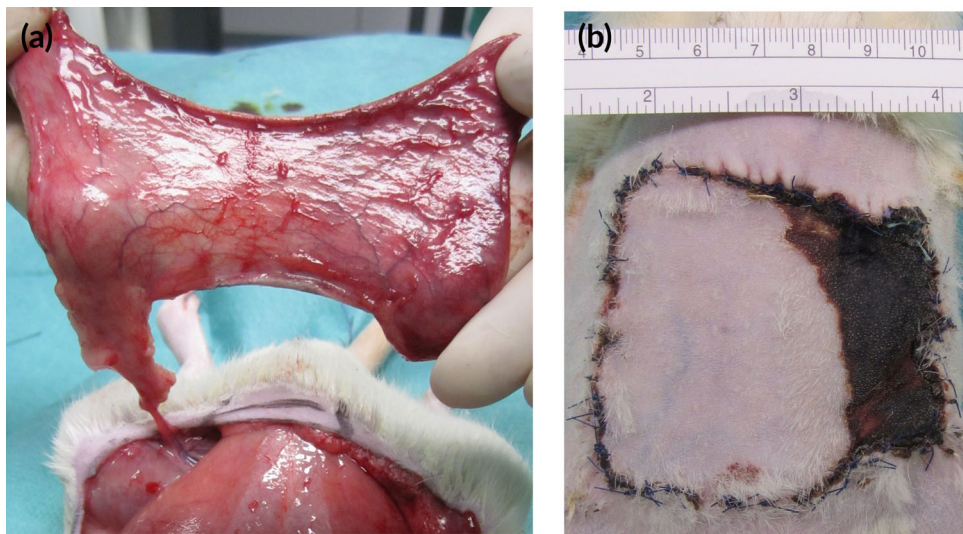


FIGURE 6 (a) A previously described epigastric flap model was used to evaluate the regenerative and angiogenic effects of the treatment protocol.⁴² After the ligation of the contralateral vascular bundle, the flap pedicle consists only of the unilateral inferior epigastric vessels. (b) The ligation of one neurovascular bundle leads to the controlled necrosis of the contralateral side of the flap tissue

4.4 | Treatment protocol

Intraoperatively, the treatment of the animals was performed using commercially available fibrin sealants (ARTISS, Baxter, Deerfield, IL, USA) as carrier substance to locally administer the dissolved freeze-dried supernatants. In the PBMCsec group, the secretome of 5×10^7 cells mixed into 2 ml (final concentration: 2.5×10^7 cells/ml) of fibrin sealant was applied evenly over the wound area between the flap and the abdominal muscular wall immediately before wound closure. In the fibrin sealant group, no PBMCsec was added to the fibrin sealant. Animals in the control group received no additional treatment during surgery.

4.5 | Digital image planimetry

The surface area of the flap including the necrotic flap area was traced onto a transparent acrylic foil, which was then photographed. Digital images were analyzed using the ImageJ software.⁵³ Measurements were performed after the surgery, on postoperative days 3 and 7. The entire flap surface area was defined by the flap borders and the flap necrosis rate was expressed as percentage of the total area. Flap areas which appeared black with hair loss, induration, and loss of skin elasticity were defined as necrotic.

4.6 | Flap perfusion measurements

The flap perfusion was measured with the LDI system preoperatively, postoperatively, and on postoperative days 3 and 7. A low intensity (2 mW) laser light beam (wavelength 632.8 nm) scans the surface of the epigastric flap skin and generates a 2-dimensional image of flap perfusion. Moving blood cells shift the frequency of the laser light according to the Doppler principle. This effect is converted into a color-coded image. The LDI scan modulus was set at 10 ms/pixel, and

the resolution at 256×256 pixels. All laser scans were performed without skin contact at a standardized working distance of 20 cm. Flap perfusion was expressed in arbitrary perfusion units (PU) by the analysis software (Moor Instruments Ltd.). Perfusion was calculated as the mean of the PU for each of the 3 vertical zones: Vital zone, transition zone, and ischemic zone.

4.7 | Macroscopic evaluation

Flaps were evaluated clinically on day 7 by a blinded observer. After a cranial incision, assessments were performed for seroma volume, flap adherence to the wound bed (0 = no adherence of the flap to the underlying abdominal wall, 1 = less than 50% of the flap area is adherent to the abdominal wall, 2 = 50% to less than 100% of the flap area is adherent to the abdominal wall, 3 = full adherence of the flap to the abdominal wall) and edema formation using a grading scale (0 = no visible edema, 1 = minimal signs of edema of the flap, 2 = moderate edema of the flap, 3 = maximum edema of the entire flap) as established previously (Table 2).⁴² Seroma fluid between the muscular abdominal wall and the flap was aspirated with a syringe and measured.

4.8 | Immunohistochemistry

Full-thickness sections from epigastric skin flaps (border from vital to necrotic area) were used for immunohistochemical (IHC) analyses. IHC staining of vascular endothelial cells was performed using an antibody against von Willebrand Factor (vWF; Agilent, Santa Clara, CA) to visualize blood vessels. To evaluate the formation of lymphatic vessels, the tissue sections were also stained for VEGF-receptor-3 (Flt-4, Santa Cruz Biotechnology, Dallax, TX). Staining was performed on paraffin-embedded tissues after antigen retrieval by boiling in citrate-buffer (pH = 6, Dako, Glostrup, Denmark) in a microwave for 5 min.

TABLE 2 The clinical scoring systems for flap adherence and tissue edema

	Flap adherence	Tissue edema
Grading		
0	No adherence of the flap to the underlying abdominal wall	No visible edema
1	Less than 50% of the flap area is adherent to the abdominal wall	Minimal signs of edema of the flap
2	50% to less than 100% of the flap area is adherent to the abdominal wall	Moderate edema of the flap
3	Full adherence of the flap to the abdominal wall	Maximum edema of the entire flap

After blocking the sections with 10% normal goat serum for 1 hr, the slides were incubated overnight in a humidified chamber at 4°C with the antibodies or isotype-matched control (Abcam) antibody diluted in PBS containing 2% bovine serum albumin (BSA) and 10% goat serum. To visualize the stainings, sections were incubated with a horseradish peroxidase-linked secondary antibody in PBS containing 2% BSA and 10% normal goat serum for 1 hr, followed by incubation with DAB Chromogen tablets (Dako). After washing, nuclear staining was performed by incubation with hematoxylin for 10 s. Slides were mounted with Fluoprep (bioMérieux, Marcy l'Etoile, France). vWF-positive vessels were counted in four fields (200× magnification) per slide by a blinded observer. Flt-4-positive cells were quantitatively analyzed in four fields (200× magnification) by tissue cytometry using the HistoQuest™ software (TissueGnostics, Vienna, Austria).

4.9 | Statistical analysis

We used IBM SPSS Statistics 24.0 (IBM, Armonk, NY) for data analysis. In case of a normal distribution of a metric variable, the Student's *t*-test was used to compare groups. Otherwise, the nonparametric Mann-Whitney U-Test was used. If not stated otherwise, results are given as mean ± standard deviation (SD). In all calculations, a *p*-value <.05 was considered statistically significant. The *p*-values were not adjusted for multiple comparisons.

5 | CONCLUSIONS

In conclusion, we demonstrated a significantly reduced necrosis rate in combination with increased blood vessel density after a single, intraoperative application of the secretome derived from γ -irradiated, stressed PBMCs in a rodent epigastric flap model. GMP-compliant production of PBMCsec yields a consistent composition of the cell-derived secretome as a biological medicinal product and recent studies have demonstrated its safety and tolerability.^{40,47,48} Our study identified a beneficial combinatory effect of PBMCsec and fibrin glue

for flap survival of marginally perfused tissue areas, which might therefore represent a powerful tool for reconstructive and aesthetic surgeons.

ACKNOWLEDGMENTS

This work was funded by the Medical Scientific Fund of the Mayor of the City of Vienna, the Ludwig Boltzmann Institute for Experimental and Clinical Traumatology, and the Laboratory for Cardiac and Thoracic Diagnosis and Regeneration and Applied Immunology.

CONFLICT OF INTEREST

The Medical University of Vienna has claimed financial interest and Hendrik J. Ankersmit holds patents related to this work and is a shareholder of Aposcience AG. All other authors declare no potential conflict of interest.

ORCID

Stefan Hacker  <https://orcid.org/0000-0002-6376-4687>

REFERENCES

1. Busnardo FF, Coltro PS, Oliván MV, Busnardo AP, Ferreira MC. The thoracodorsal artery perforator flap in the treatment of axillary hidradenitis suppurativa: effect on preservation of arm abduction. *Plast Reconstr Surg*. 2011;128:949-953.
2. Huemer GM, Larcher L, Schoeller T, Bauer T. The free gracilis muscle flap in achilles tendon coverage and reconstruction. *Plast Reconstr Surg*. 2012;129:910-919.
3. Lin DT, Coppit GL, Burkey BB. Use of the anterolateral thigh flap for reconstruction of the head and neck. *Curr Opin Otolaryngol Head Neck Surg*. 2004;12:300-304.
4. Kryger Z, Dogan T, Zhang F, et al. Effects of VEGF administration following ischemia on survival of the gracilis muscle flap in the rat. *Ann Plast Surg*. 1999;43:172-178.
5. Kwok AC, Agarwal JP. An analysis of free flap failure using the ACS NSQIP database. Does flap site and flap type matter? *Microsurgery*. 2017;37:531-538.
6. Thangarajah H, Yao D, Chang EI, et al. The molecular basis for impaired hypoxia-induced VEGF expression in diabetic tissues. *Proc Natl Acad Sci U S A*. 2009;106:13505-13510.
7. Valentini V, Cassoni A, Marianetti TM, et al. Diabetes as main risk factor in head and neck reconstructive surgery with free flaps. *J Craniofac Surg*. 2008;19:1080-1084.
8. Ishimaru M, Ono S, Suzuki S, Matsui H, Fushimi K, Yasunaga H. Risk factors for free flap failure in 2,846 patients with head and neck cancer: a National Database Study in Japan. *J Oral Maxillofac Surg*. 2016;74:1265-1270.
9. Caputo MP, Shabani S, Mhaskar R, McMullen C, Padhya TA, Mifsud MJ. Diabetes mellitus in major head and neck cancer surgery: systematic review and meta-analysis. *Head Neck*. 2020. doi:10.1002/hed.26349. Online ahead of print.
10. Mirabella T, Hartinger J, Lorandi C, Gentili C, van Griensven M, Cancedda R. Proangiogenic soluble factors from amniotic fluid stem cells mediate the recruitment of endothelial progenitors in a model of ischemic fasciocutaneous flap. *Stem Cells Dev*. 2012;21:2179-2188.
11. Kosko JR, Williams PB, Pratt MF. Correlation of neutrophil activation and skin flap survival in pharmacologically altered pigs. *Ann Otol Rhinol Laryngol*. 1997;106:790-794.
12. Pang CY, Forrest CR, Morris SF. Pharmacological augmentation of skin flap viability: a hypothesis to mimic the surgical delay phenomenon or a wishful thought. *Ann Plast Surg*. 1989;22:293-306.

13. Wax MK, Reh DD, Levack MM. Effect of celecoxib on fasciocutaneous flap survival and revascularization. *Arch Facial Plast Surg.* 2007;9:120-124.
14. Camargo CP, Pfann RZ, Kubrusly MS, et al. Study of the effect of hyperbaric oxygen therapy on the viability of dorsal cutaneous flaps in tobacco-exposed rats. *Aesthetic Plast Surg.* 2020;44:979-985.
15. Ellabban MA, Fattah IOA, Kader GA, et al. The effects of sildenafil and/or nitroglycerin on random-pattern skin flaps after nicotine application in rats. *Sci Rep.* 2020;10:3212.
16. Abdelfattah U, Elbanoby T, Kim EN, Park EJ, Suh HP, Hong JPJ. Effect of simvastatin use in free tissue transfer: an experimental study in a rat Epigastric free flap model. *J Reconstr Microsurg.* 2020;36:281-288.
17. Hockel M, Schlenger K, Doctrow S, Kissel T, Vaupel P. Therapeutic angiogenesis. *Arch Surg.* 1993;128:423-429.
18. Isner JM, Asahara T. Angiogenesis and vasculogenesis as therapeutic strategies for postnatal neovascularization. *J Clin Invest.* 1999;103:1231-1236.
19. Brown DM, Hong SP, Farrell CL, Pierce GF, Khouri RK. Platelet-derived growth factor BB induces functional vascular anastomoses in vivo. *Proc Natl Acad Sci U S A.* 1995;92:5920-5924.
20. Hom DB, Simplot TC, Pernel KJ, Manivel JC, Song CW. Vascular and epidermal effects of fibroblast growth factor on irradiated and nonirradiated skin flaps. *Ann Otol Rhinol Laryngol.* 2000;109:667-675.
21. Scalise A, Tucci MG, Lucarini G, et al. Local rh-VEGF administration enhances skin flap survival more than other types of rh-VEGF administration: a clinical, morphological and immunohistochemical study. *Exp Dermatol.* 2004;13:682-690.
22. Chai J, Ge J, Zou J. Effect of autologous platelet-rich plasma gel on skin flap survival. *Med Sci Monitor.* 2019;25:1611-1620.
23. Wang B, Geng Q, Hu J, Shao J, Ruan J, Zheng J. Platelet-rich plasma reduces skin flap inflammatory cells infiltration and improves survival rates through induction of angiogenesis: an experiment in rabbits. *J Plast Surg Hand Surg.* 2016;50:239-245.
24. Mittermayr R, Morton T, Hofmann M, Helgerson S, van Griensven M, Redl H. Sustained (rh)VEGF(165) release from a sprayed fibrin biomatrix induces angiogenesis, up-regulation of endogenous VEGF-R2, and reduces ischemic flap necrosis. *Wound Repair Regen.* 2008;16:542-550.
25. Jorgensen S, Bascom DA, Partasafas A, Wax MK. The effect of 2 sealants (FloSeal and Tisseel) on fasciocutaneous flap revascularization. *Arch Facial Plast Surg.* 2003;5:399-402.
26. Mittermayr R, Slezak P, Haffner N, et al. Controlled release of fibrin matrix-conjugated platelet derived growth factor improves ischemic tissue regeneration by functional angiogenesis. *Acta Biomater.* 2016;29:11-20.
27. Michlits W, Mittermayr R, Schafer R, Redl H, Aharinejad S. Fibrin-embedded administration of VEGF plasmid enhances skin flap survival. *Wound Repair Regen.* 2007;15:360-367.
28. Giordano S, Koskivuo I, Suominen E, Verajankorva E. Tissue sealants may reduce haematoma and complications in face-lifts: a meta-analysis of comparative studies. *J Plast Reconstr Aesthet Surg.* 2017;70:297-306.
29. Pavo N, Zimmermann M, Pils D, et al. Long-acting beneficial effect of percutaneously intramyocardially delivered secretome of apoptotic peripheral blood cells on porcine chronic ischemic left ventricular dysfunction. *Biomaterials.* 2014;35:3541-3550.
30. Lichtenauer M, Mildner M, Hoetzenecker K, et al. Secretome of apoptotic peripheral blood cells (APOSEC) confers cytoprotection to cardiomyocytes and inhibits tissue remodelling after acute myocardial infarction: a preclinical study. *Basic Res Cardiol.* 2011;106:1283-1297.
31. Beer L, Zimmermann M, Mitterbauer A, et al. Analysis of the Secretome of apoptotic peripheral blood mononuclear cells: impact of released proteins and Exosomes for tissue regeneration. *Sci Rep.* 2015;5:16662.
32. Simader E, Beer L, Laggner M, et al. Tissue-regenerative potential of the secretome of gamma-irradiated peripheral blood mononuclear cells is mediated via TNFRSF1B-induced necroptosis. *Cell Death Dis.* 2019;10:729.
33. Wagner T, Traxler D, Simader E, et al. Different pro-angiogenic potential of gamma-irradiated PBMC-derived secretome and its sub-fractions. *Sci Rep.* 2018;8:18016.
34. Beer L, Mildner M, Gyongyosi M, Ankersmit HJ. Peripheral blood mononuclear cell secretome for tissue repair. *Apoptosis.* 2016;21:1336-1353.
35. Mildner M, Hacker S, Haider T, et al. Secretome of peripheral blood mononuclear cells enhances wound healing. *PLoS One.* 2013;8:e60103.
36. Hacker S, Mittermayr R, Nickl S, et al. Paracrine factors from irradiated peripheral blood mononuclear cells improve skin regeneration and angiogenesis in a porcine burn model. *Sci Rep.* 2016;6:25168.
37. Hoetzenecker K, Zimmermann M, Hoetzenecker W, et al. Mononuclear cell secretome protects from experimental autoimmune myocarditis. *Eur Heart J.* 2015;36:676-685.
38. Hoetzenecker K, Assinger A, Lichtenauer M, et al. Secretome of apoptotic peripheral blood cells (APOSEC) attenuates microvascular obstruction in a porcine closed chest reperfused acute myocardial infarction model: role of platelet aggregation and vasodilation. *Basic Res Cardiol.* 2012;107:292.
39. Haider T, Hoftberger R, Ruger B, et al. The secretome of apoptotic human peripheral blood mononuclear cells attenuates secondary damage following spinal cord injury in rats. *Exp Neurol.* 2015;267:230-242.
40. Simader E, Traxler D, Kasiri MM, et al. Safety and tolerability of topically administered autologous, apoptotic PBMC secretome (APOSEC) in dermal wounds: a randomized phase 1 trial (MARSYAS I). *Sci Rep.* 2017;7:6216.
41. Spear SL, Ducic I, Cuoco F, Hannan C. The effect of smoking on flap and donor-site complications in pedicled TRAM breast reconstruction. *Plast Reconstr Surg.* 2005;116:1873-1880.
42. Mittermayr R, Hartinger J, Antonic V, et al. Extracorporeal shock wave therapy (ESWT) minimizes ischemic tissue necrosis irrespective of application time and promotes tissue revascularization by stimulating angiogenesis. *Ann Surg.* 2011;253:1024-1032.
43. Reichenberger MA, Mueller W, Schafer A, et al. Fibrin-embedded adipose derived stem cells enhance skin flap survival. *Stem Cell Rev Rep.* 2012;8:844-853.
44. Mooney E, Loh C, Pu LL, ASPSPSEF Technology Assessment Committee. The use of fibrin glue in plastic surgery. *Plast Reconstr Surg.* 2009;124:989-992.
45. Kim JT, Kim YH, Kim SW. Effect of fibrin sealant in positioning and stabilizing microvascular pedicle: a comparative study. *Microsurgery.* 2017;37:406-409.
46. Mabrouk AA, Helal HA, Al Mekkawy SF, Mahmoud NA, Abdel-Salam AM. Fibrin sealant and lipoabdominoplasty in obese grade 1 and 2 patients. *Arch Plast Surg.* 2013;40:621-626.
47. Laggner M, Gugerell A, Bachmann C, et al. Reproducibility of GMP-compliant production of therapeutic stressed peripheral blood mononuclear cell-derived secretomes, a novel class of biological medicinal products. *Stem Cell Research & Therapy.* 2020;11:9.
48. Wuschko S, Gugerell A, Chabicovsky M, et al. Toxicological testing of allogeneic secretome derived from peripheral mononuclear cells (APOSEC): a novel cell-free therapeutic agent in skin disease. *Sci Rep.* 2019;9:5598.
49. Du W, Wu PF, Qing LM, et al. Systemic and flap inflammatory response associates with thrombosis in flap venous crisis. *Inflammation.* 2015;38:298-304.
50. Laggner M, Copic D, Nemeč L, et al. Therapeutic potential of lipids obtained from gamma-irradiated PBMCs in dendritic cell-mediated skin inflammation. *EBioMedicine.* 2020;55:102774.

51. Altmann P, Mildner M, Haider T, et al. Secretomes of apoptotic mononuclear cells ameliorate neurological damage in rats with focal ischemia. *F1000Research*. 2014;3:131.
52. Kasiri MM, Beer L, Nemeč L, et al. Dying blood mononuclear cell secretome exerts antimicrobial activity. *Eur J Clin Invest*. 2016;46: 853-863.
53. Schneider CA, Rasband WS, Eliceiri KW. NIH image to ImageJ: 25 years of image analysis. *Nat Methods*. 2012;9:671-675.

How to cite this article: Hacker S, Mittermayr R, Traxler D, et al. The secretome of stressed peripheral blood mononuclear cells increases tissue survival in a rodent epigastric flap model. *Bioeng Transl Med*. 2020;e10186. <https://doi.org/10.1002/btm2.10186>